UCRL-JC-132825
Preprint

Corrosion of Candidate Container Materials by Yucca Mountain Bacteria

Tiangan Lian
Sue Martin
Denny Jones
Angel Rivera
Joanne Horn

This paper was prepared for submittal to
NACE Annual Conference and Exposition
CORROSION/99
San Antonio, TX
April 25-30, 1999

January 1999

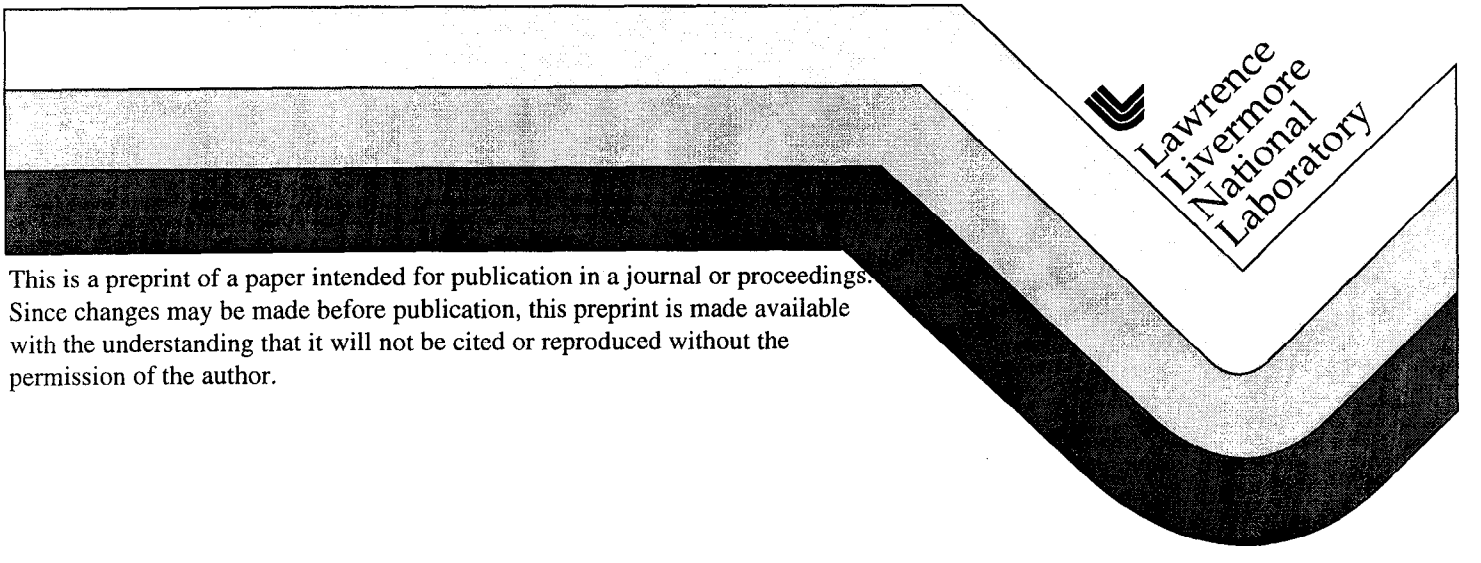

NACE Annual Conference and Exposition
CORROSION/99, Paper #99476
San Antonio, TX
April 25-30, 1999

CORROSION OF CANDIDATE CONTAINER MATERIALS BY YUCCA MOUNTAIN BACTERIA

Tiangan Lian
Sue Martin
Denny Jones*
Angel Rivera
Joanne Horn

Lawrence Livermore National Laboratory
Livermore, CA 94550

***Department of Chemical & Metallurgical Engineering**
University of Nevada-Reno
Reno, Nevada 89557

ABSTRACT

Several candidate container materials have been studied in modified Yucca Mountain (YM) ground water in the presence or absence of YM bacteria. YM bacteria increased corrosion rates by 5-6 fold in UNS G10200 carbon steel, and nearly 100-fold in UNS N04400 Ni-Cu alloy. YM bacteria caused microbiologically influenced corrosion (MIC) through de-alloying or Ni-depletion of Ni-Cu alloy as evidenced by scanning electronic microscopy (SEM) and inductively coupled plasma spectroscopy (ICP) analysis. MIC rates of more corrosion-resistant alloys such as UNS N06022 Ni-Cr-Mo-W alloy, UNS N06625 Ni-Cr-Mo alloy, and UNS S30400 stainless steel were measured below 0.05 μm/yr, however YM bacteria affected depletion of Cr and Fe relative to Ni in these materials. The chemical change on the metal surface caused by depletion was characterized in anodic polarization behavior. The anodic polarization behavior of depleted Ni-based alloys was similar to that of pure Ni.

Key words: MIC, container materials, YM bacteria, de-alloying, Ni-depletion, Cr-depletion, polarization resistance, anodic polarization,

INTRODUCTION

The long-term performance of the engineered barrier system is a crucial factor in assessing the degree of containment of nuclear waste by a potential geological repository at Yucca Mountain, Nevada. Currently, a multi-layer container is being designed to safely constrain emplaced nuclear wastes for at

least 10,000 years. Over the long term required for safe containment of wastes, the interaction between the YM underground environment and waste containers will have a significant impact on the integrity of the engineered barrier system, and thus on the over-all performance of the repository system.

MIC may be a significant factor contributing to container corrosion. Previous characterization of bacterial isolates derived from YM geologic materials showed that many possessed biochemical activities associated with MIC.[1],[2] Extant YM microorganisms have been shown to be capable of: iron oxidization, acid production, sulfate reduction, and the generation of slime, all activities associated with MIC.[3] Since the potential of MIC in waste package materials has been established, the aim of these studies has been to determine the microbial contribution to waste package corrosion for the purpose of assessing the long-term containment of nuclear wastes. We have used both electrochemical and chemical analyses to both define overall MIC rates, and evaluate MIC mechanisms of corrosion on candidate waste package materials. Candidate alloys were exposed to YM microbes in simulated YM ground water, or left sterile for comparison. DC electrochemical polarization techniques were used to assess corrosion rates and mechanisms. Chemical analysis of the bulk aqueous fluid surrounding coupons, and examination of the coupon surfaces further contributed to assessing microbial effects on corrosion by comparing surfaces incubated with YM bacteria to those left sterile.

EXPERIMENTAL PROCEDURES

Figure 1 depicts the schematic diagram of the corrosion cell designed to allow the interaction between test specimens, the test medium, and introduced microorganisms, as well as facilitate implementation of electrochemical DC polarization. A cylindrical glass flange with O-ring seals was clamped to a sheet specimen that acted as a working electrode and formed the bottom of the vessel. The corrosion cell allowed an exposed area of 28.3 cm^2 on the coupon specimen (or working electrode). A platinum wire was used as an auxiliary electrode, and a commercial saturated calomel electrode (SCE) was used as a reference electrode.

The materials tested included UNS G10200 (carbon steel, abbreviated as C1020 throughout the paper), UNS N04400 (Ni-Cu alloy, as M400), UNS S30400 (Type 304 stainless steel, as 304SS), UNS N06625 (Ni-Cr-Mo alloy, as I625) and UNS N06022 (Ni-Cr-Mo-W alloy, as C-22). In the multi-layer container design, C1020 and M400 are considered as corrosion allowance materials (CAMs) to be used in outer layer, while C-22, I625 and 304SS are considered as corrosion resistance materials (CRMs) to be used in inner layer. The chemical compositions of test materials are given in Table 1. The specimens were received as flat circular disc-shaped coupons (2 3/4" or 7 cm diameter). The exposed side of coupons was wet-polished with abrasive paper progressively to 600-grit, cleaned with acetone and distilled water, and the assembled cells were then sterilized by autoclaving.

12 strains of YM bacteria, including acid, slime, and sulfide producers, as well as iron-oxidizing bacteria (Table 2) were mixed and applied to coupon surfaces. Microbial cell densities were established before aseptically combining and spreading a defined number (at least 10^8 bacterial cells of each strain) of all isolates on specimens which were air dried before they were exposed to growth media in corrosion cells. The growth medium was 450 ml of R2 low-nutrient formulation bacterial growth media,[3] supplemented with 0.5% glucose and 0.75% protease peptone #3 (Difco, Detroit, MI) in 100X simulated J-13 well water (water from the vicinity of the YM site[4]). All vessels were incubated at room temperature (approximately 22°C). An identical set of corrosion cells without bacteria were maintained

in a sterile condition for comparison. Triplicates of each type of corrosion cell were constructed and analyzed to provide analysis of experimental variation.

The DC linear polarization technique was periodically used to conduct polarization resistance (R_p) measurements in corrosion vessels. A potentiostat (EG&G Model 283) performed potential scans from 20 mV lower than the corrosion potential (E_{corr}) to 20 mV greater than E_{corr} at a scan rate of 0.04 mV/sec. The R_p was calculated by the EG&G Model 252/352 Softcorr II software. Corrosion rates as current density (i_{corr}) in $\mu A/cm^2$ were calculated from the measured R_p in $10^{-6}\cdot\Omega\cdot cm^2$,[5] using the following equation:

$$i_{corr} = B/R_p \quad (1)$$

where

$$B = \beta_a\beta_c/2.303\ (\beta_a + \beta_c) \quad (2)$$

β_a and β_c are known as anodic and cathodic Tafel constants (activation polarization), respectively. β_a and β_c can be determined experimentally by polarization measurement. However, undetermined β_a and β_c do not cause significant error in calculated corrosion rate, and approximate values of $\beta_a = \beta_c = 0.1$ V/decade are usually used when β_a and β_c are unknown.

Polarization measurements gave $\beta_a = \beta_c = 0.15$ V/decade for the sterile carbon steel C1020, and $\beta_a = 0.035$V/decade and $\beta_c = 0.315$V/decade for C1020 in the inoculated cells. For the rest of materials, the corrosion rate calculations were based on $\beta_a = \beta_c = 0.1$ V/decade. i_{corr} was then converted to corrosion rate (r) in micrometers per year (μm/yr) as:

$$r = 3.27\ i_{corr}\ a/(n\ D) \quad (3)$$

where a is atomic weight, n is equivalent number, and D is density. The corrosion rate monitoring ran for approximately 5 month.

Anodic polarization measurements were conducted in selective cells after 5-months of incubation. A scan rate at 600mV per hour was used. Aqueous spent media sampled from the cells in which no extensive anodic or cathodic polarization had been performed, were analyzed by using ICP to determine the dissolution of metal alloying elements. SEM with Energy Dispersive X-Ray Analysis (EDAX) was used for post-exposure analysis of specimen surfaces.

RESULTS AND OBSERVATIONS

Corrosion of CAMs -- C1020 and M400

Corrosion rates of C1020 and M400 exposed to supplemented J-13 water were significantly increased by the presence of YM bacteria. The corrosion rate of C1020 was increased by about 5-6-fold, while a 100-fold increase in corrosion rate was observed on M400 due to microbial activity (Figure 2). The observed MIC rate of M400, as expected, was lower than that of C1020. However, the corrosion rate of M400 was increased nearly 3-fold during the first two weeks of incubation, while the corrosion rate of C1020 was decreased. Thus, there was an initial 80-fold differential in MIC corrosion rates between the two materials (0.31 μm/y for M400 and 24.89 μm/y for C1020). However, this difference

was decreased to 7-8 folds after steady state was achieved (approximately 1.02 μm/y for M400 and 7.62 μm/y for C1020). Under sterile conditions without YM bacteria, M400 was more than 100 times more corrosion resistant than sterile C1020 under these experimental conditions. However, the presence of YM bacteria resulted in a ten-fold decrease of this differential, whereby the corrosion susceptibility was enhanced in both materials. Thus, both C1020 and M400 displayed the effects of YM bacteria to increase their corrosion rates.

After 5-months exposure in supplemented J-13 waters, with and without YM bacteria, M400 coupons were removed and their surfaces were analyzed. The gross appearance of the M400 coupon incubated under sterile conditions remained unchanged from its initial appearance before exposure [Figure 3(b)]. However, the M400 coupon incubated under inoculated conditions with YM bacteria displayed a discoloration [Figure 3(a)]. This inoculated coupon was covered with an accretion of bacteria, or bio-film, mixed with corrosion products. Further inspection of the surface under the bio-film using SEM and EDAX, revealed de-alloying of the M400, leaving behind a deteriorated substratum depleted of Ni (Figure 4).

Elemental analysis of aqueous spent medium after 5-months incubation by ICP in the corrosion cells containing a M400 coupon and YM bacteria confirmed preferential Ni dissolution from M400 (Table 3). The Ni:Cu ratio in the solution incubated with an inoculated M400 coupon is 18.5:1 [Table 3 (a)], which is significantly greater than the ratio of 70:30 Ni:Cu in the original composition of M400 (Table 1). In contrast, the solution incubated with sterile M400 coupons showed minimal dissolution of Fe, Cu, and Ni. Elemental analysis of supplemented, spent J13 medium incubated with an inoculated C1020 coupon by ICP also shows that YM bacteria caused a significant amount of Fe dissolution from C1020 [Table 3(a)].

Anodic polarization measurements show the electrochemical behavior of M400 and C1020 after 5-months exposure in the corrosion cells. An active anodic polarization behavior was observed on C1020 after exposure to YM bacteria for 5-months (Figure 5), while previous experimental data showed an active-passive behavior on C1020 exposed to this same test medium with no YM bacteria [2]. An anodic polarization scan of M400 exposed to the medium without the addition of YM bacteria resulted in pitting of the coupon surface, as evidenced by a breakdown potential in the polarization curve (Figure 5). However, no pitting was generated during an anodic polarization scan of an M400 coupon incubated with YM bacteria. The anodic polarization curve shows an anodic peak, but no breakdown potentials. After the anodic polarization, a Cu-colored film covered the Pt-wire (served as auxiliary electrode). A similar film was also observed to cover the M400 coupon surface after cathodic polarization measurements had been performed (data not shown). This observation indicates that Cu was initially dissolved into solution, then reduced, and re-deposited on the surface of the coupon, resulting in the observed discoloration of microbiologically exposed M400.

Corrosion of CRMs -- 304SS, I625 and C-22

Corrosion rates of C-22, I625, and 304SS inoculated with YM bacteria in amended J-13 water were all below 0.05 μm/yr, as determined by polarization resistance (Figure 6). The MIC rate of 304SS was observed to be the highest among the three corrosion resistance materials (CRMs) tested. All CRM coupon surfaces did not show gross alterations in their appearance after the 5-month incubation period. Although MIC rates were comparatively low for the CRMs tested, there was a detectable and significant data in (Figure 6). YM bacteria increased corrosion rates by more than 100-fold in 304SS, 4-5-fold in I625 and about 2-fold in C-22. It appears that C-22 is least susceptible to MIC of the three CRMs tested.

Elemental analysis by ICP of aqueous spent media sampled from several cells after 5-months incubation showed depletion of Cr in all CRMs exposed to YM bacteria [Table 3(b)]. A ratio of Cr:Ni dissolved in the solution incubated with bacteria and 304SS was determined to be approximately 25:1, compared to the Cr:Ni ratio of 18:8 in the original composition of 304SS. Nearly 10:1 of Cr:Ni ratio was observed in the solution incubated with either I625 or C-22 and YM bacteria, compared to the Cr:Ni ratio of about 3:1 in original composition of I625 and C-22. In stark contrast, no Cr, Ni, or Mo dissolution from CRMs was detected in solutions incubated in the absence of YM bacteria after 5-months incubation.

Elemental analysis by ICP revealed some minor dissolution of Fe in all three CRMs after 5-months incubation in the presence or absence of YM bacteria. YM bacteria had little apparent effect on Fe-depletion of I625 and Alloy 22, but, when 100X J13 media concentrations of Fe are taken into account microbial activity was appeared to increase Fe-depletion in 304SS by nearly 5-fold (Table 3).

Anodic polarization scans were not able to initiate pitting in CRMs with or without YM bacteria added to corrosion cells. However, the presence of YM bacteria did result in an alteration of the anodic polarization behavior of CRMs (Figure 7). Anodic polarization curves generated in the presence of YM bacteria were significantly shifted down and to the right compared to the curves generated in system without YM bacteria. In the sterile environments, an anodic peak was observed in the polarization curves of I625 and C-22, which was not apparent when YM bacteria were present (Figure 7).

DISCUSSION

The results described here have shown that YM bacteria caused varying degrees of de-alloying or preferential dissolution of alloy components in all tested candidate materials, except carbon steel. The de-alloying of Ni from M400 by YM bacteria resulted in discoloration of the coupon and Cu-enrichment on the surface, as indicated by EDAX and ICP analysis. Although no discoloration was observed in CRMs, the elemental analytical results indicated Cr-depletion in these materials.

Two mechanisms of de-alloying of M400 have been proposed:[6]

(i) Simultaneous dissolution of both the Ni and Cu components of the alloy followed by re-deposition of one element on the metal surface.

(ii) Selective dissolution of a single element from the crystal lattice.

Re-deposition of Cu on the Pt auxiliary electrode during anodic polarization, and on M400 coupon surface during cathodic polarization indicates that Cu was initially dissolved into solution, then reduced, and re-deposited on the surface of the coupon, resulting in the observed discoloration of microbiologically exposed Alloy 400. Thus, our observations support the mechanistic model of Alloy 400 microbial de-alloying as an initial simultaneous dissolution of Cu, Ni, and Fe brought about by YM bacterial activities, with a later reduction of dissolved Cu and deposition of the elemental Cu on the metal surface. The observed "preferential" Ni dissolution from M400, was evident only after Cu precipitation had taken place, since initially both Cu and Ni were in solution, but subsequent Cu precipitation resulted in higher concentrations of Ni than Cu in solution. Many types of bacteria are known to carry out metal transformations, especially reductions of cationic metal ions. YM bacteria contained in corrosion cells may thus also influence the reduction of dissolved Cu ions, as well as their

initial dissolution. Taken together, our results demonstrate that, YM bacteria clearly contributed to simultaneous dissolution of Cu and Ni from M400 into the solution, and may have directly or indirectly caused reduction and precipitation of dissolved Cu.

It is not clear precisely how YM bacteria are involved in the above processes. Adding Cu to Ni-based alloys improves the corrosion resistance of Ni to non-oxidizing solutions. However, Cu can be attacked rapidly in sulfide-containing solutions, and MIC of Cu caused by sulfide-producing bacteria has been reported.[7] Inclusion of YM-derived sulfide-producing organisms in these experiments may have thus provided favorable conditions for the dissolution of Cu..

In CRMs, de-alloying was caused by selective dissolution of Cr and Fe from the bulk alloy. Nickel is a more noble metal than chromium or iron in most electrochemical systems, and Ni-Cr or Ni-Fe galvanic couples can accelerate preferential depletion of Cr or Fe from Ni-containing alloys. The presence of YM bacterial activities may directly or indirectly accelerate this type of de-alloying. The microbes may have contributed to creating conditions to enhance the galvanic effects and dissolution of the active metals. It is noteworthy that Geesey et. al.[8] reported significant depletion of Cr and Fe relative to Ni on the surface 316L stainless steel caused by biofilm-forming bacteria. Cr depletion was observed in the near-surface region of the oxide film at grain boundaries. The chemical change may weaken the oxide film to allow aggressive species in the solution greater access to the underlying bulk alloy, and thereby facilitate pitting or other forms of localized attack.

The shift of anodic polarization curves demonstrates that YM bacteria caused a chemical change in the surface of tested candidate materials. In the case of M400, the addition of an anodic peak in the anodic polarization curve indicates a higher Cu content on the metal surface, as confirmed by EDS analysis, in agreement with findings reported by Beccaria and Crousia.[6] In I625 and C-22 with YM bacteria, the anodic polarization curves appear more like the one from pure Ni, perhaps reflecting the depletion of Cr and resulting enrichment of Ni on the coupon surface. It is not presently clear why an anodic peak was observed in anodic polarization curves with no YM bacteria.

CONCLUSIONS

The following conclusions can be drawn from the experimental results of this investigation:

(1) YM bacteria significantly increased corrosion rates of UNS G10200 carbon steel and UNS N04400 Ni-Cu alloy. A MIC-caused corrosion rate increase of 5-6-fold in UNS G10200, and nearly 100-fold in UNS N04400 were observed after 5-months exposure to simulated YM ground water in the presence of YM bacteria.

(2) UNS N04400 Ni-Cu alloy was susceptible to MIC in YM repository environments. YM bacteria caused de-alloying of UNS N04400. Simultaneous dissolution of Cu and Ni from UNS N04400 was caused by YM bacterial activities, and ensuing Ni-depletion was driven by copper re-deposition onto metal surface.

(3) Corrosion rates of UNS N06022 Ni-Cr-Mo-W alloy, UNS N06625 Ni-Cr-Mo alloy and UNS S30400 Type 304 stainless steel exposed to YM microbial environment were measured below 0.05 μm/yr. UNS N06022 showed the least susceptibility to MIC, while corrosion rate of UNS S30400 were increased100-fold by YM bacteria.

(4) Analysis of spent aqueous media revealed Cr and Fe-depletion relative to Ni in CRMs. The depletion caused chemical changes in the near surface region of CRMs as indicated by anodic polarization behavior. With depletion of Cr and Fe, a Ni-enriched surface was characterized in anodic polarization curves.

ACKNOWLEDGEMENTS

The authors gratefully acknowledge the expert technical assistance contributed by Michael Davis in performing these experiments. This work was performed under the auspices of the U.S. Department of Energy by Lawrence Livermore National Laboratory under Contract W-7405-ENG-48, and was supported by the Yucca Mountain Site Characterization Project, LLNL.

REFERENCES

1. J. Horn, M. Davis, S, Martin, T, Lian, and D. Jones. "Assessing Microbiologically Induced Corrosion of Waste Package Alloys in the Yucca Mountain Repository," The 6th International Conference on Nuclear Engineering, Paper No. #6267, San Diego, CA, 1998.

2. J. Horn, A. Rivera, T. Lian, and D. Jones. "MIC Evaluation and Testing for the Yucca Mountain Repository," CORROSIO/98, Paper No. #152, (Houston, TX: NACE International, 1998)

3. D. J. Resoner and E. E. Geldreich, APPL. ENVIRON. MICROBIOL. 49, pp.1, 1985.

4. J. M. Delaney. "Reaction of Topopah Spring Tuff with Water: A Geochemical Modeling Approach Using the EQ3/6 Reaction Path Code," UCID Report #53631, Lawrence Livermore Natl. Laboratory, Livermore CA, Nov. 1985.

5. M. Stern and A. L. Geary, JOURNAL OF ELECTROCHEMICAL SOCIETY, Vol. 104, pp. 56, 1957.

6. A. M. Beccaria and J. Crousier. "Dealloying of Cu-Ni Alloys in Natural Sea Water," British Corrosion Journal, Vol. 24, No. 1, pp. 49-52, 1989.

7. M. B. McNeil, J. M. Jones, and B. J. Little. "Production of Sulfide Minerals by Sulfate Reducing Bacteria During Microbiologically Influenced Corrosion of Copper," CORROSION, Vol. 47, No. 9, pp. 674-677, 1991.

8. G. G. Geesey, R. J. Gillis, R. Avci, D. Daly, M. Hamilton, P. Shope and G. Harkin. "The Influence of Surface Features on Bacterial Colonization and Subsequent substratum Chemical Changes of 316L Stainless Steel," CORROSION SCIENCE, Vol. 38, No. 1, pp. 73-95, 1996

TABLE 1
CHEMICAL COMPOSITION OF CANDIDATE CONTAINER MATERIALS

UNS G10200 (abbreviated as C1020):

C (%)	Mn (%)	P (%)	S (%)	Fe (%)
0.20	0.47	0.012	0.013	99.197

UNS N04400 (abbreviated as M400):

C (%)	Mn (%)	Fe (%)	S (%)	Si (%)	Cu (%)	Ni (%)	Al (%)
0.12	0.99	1.68	0.010	0.15	31.29	65.75	0.005

UNS S30400 (abbreviated as 304SS):

C (%)	Mn (%)	P (%)	S (%)	Si (%)	Cr (%)	Ni (%)	Mo (%)	Cu (%)	N (%)	Fe (%)
0.07	1.85	0.28	0.01	0.49	18.24	8.16	0.15	0.49	0.07	70.19

UNS N06625 (abbreviated as I625):

C (%)	Mn (%)	Fe (%)	S (%)	Si (%)	Ni (%)	Cr (%)	Al (%)	Ti (%)	Mo (%)	P (%)	Cb+TA (%)
0.01	0.06	3.19	0.001	0.19	62.06	21.81	0.22	0.25	8.77	0.005	3.43

UNS N06022 (abbreviated as C-22):

C (%)	Mn (%)	S (%)	Co (%)	Mo (%)	Si (%)	Cr (%)	W (%)	V (%)	Fe (%)	P (%)	Ni (%)
0.002	0.260	0.001	0.510	13.400	0.025	21.580	2.820	0.150	3.950	0.012	57.29

TABLE 2
LIST OF YM MICROORGANISMS TESTED IN THIS EXPERIMENT

Strain #	**Species Identification**	**Classification**
ESF-71h-RT-4	*Flavobacterium esteroaaromaticum*	Acid producer
ESF-C1	*Cellulomonas flavigena*	Acid producer
LB-71h-50-3	*Bacillus*	Acid producer
Lban-U7	Uncharacterized	Acid producer
LB-C1	Uncharacterized	Slime producer
LB-71h-50-4	*Bacillus subtilus*	Slime producer
LB-71h-50-6	*Bacills sp.*	Slime producer
LB-71h-RT-15	*Pseudomonas pseudoflava*	Slime producer
Lban-U3	*Bacillus pantothentics*	Slime producer
68	Uncharacterized	Iron oxidizer
69	Uncharacterized	Iron oxidizer
	SRB's collected from YM site	Sulfate reducer

TABLE 3
DISSOLUTION OF METALS IN MEDIA AFTER 5-MONTH EXPOSURE TO YM BACTERIA

(a). Cells containing C1020 or M400

Vessel conditions/Material	Cu (mg/l)	Fe (mg/l)	Ni (mg/l)
Unexposed J-13 supplemented medium	n.d.*	0.25	n.d.
Bacteria + C1020	n.d.	16.50	n.d.
Sterile M400	0.06	0.25	0.09
Bacteria + M400	1.0	0.40	18.5

* not detectable

(b). Cells containing 304SS, I625, or C-22

Vessel conditions/Material	Fe (mg/l)	Cr (mg/l)	Ni (mg/l)	Mo (mg/l)
Unexposed J-13 supplemented medium	0.25	n.d.*	n.d.	n.d.
Sterile 304SS	0.31	n.d.	n.d.	n.d.
Bacteria + 304SS	0.57	1.03	0.04	n.d.
Sterile I625	0.31	n.d.	n.d.	n.d.
Bacteria + I625	0.33	1.07	0.12	n.d.
Sterile C-22	0.42	n.d.	n.d.	n.d.
Bacteria + C-22	0.32	1.05	0.1	n.d.

*not detectable

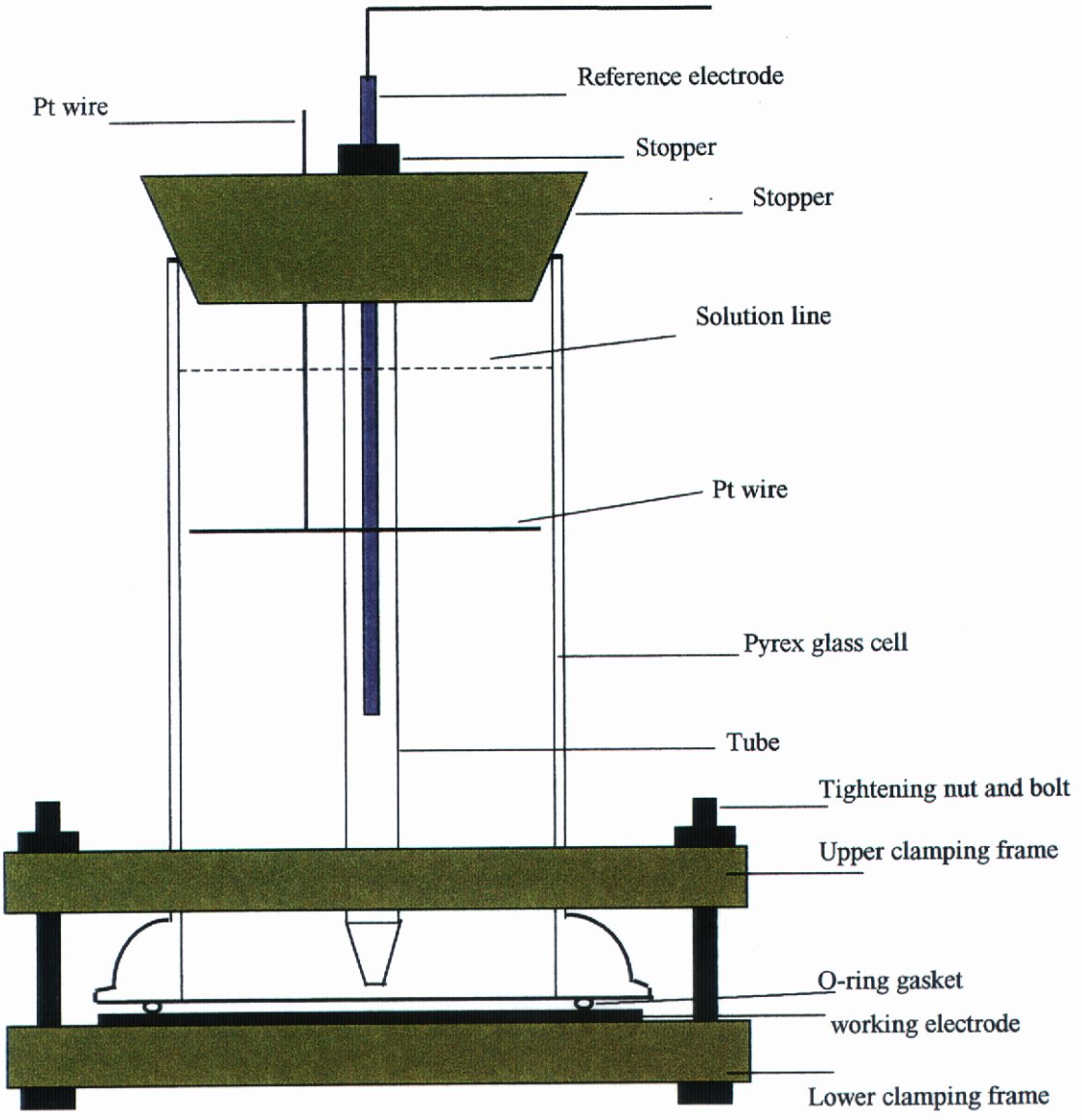

FIGURE 1: Electrochemical cell configuration.

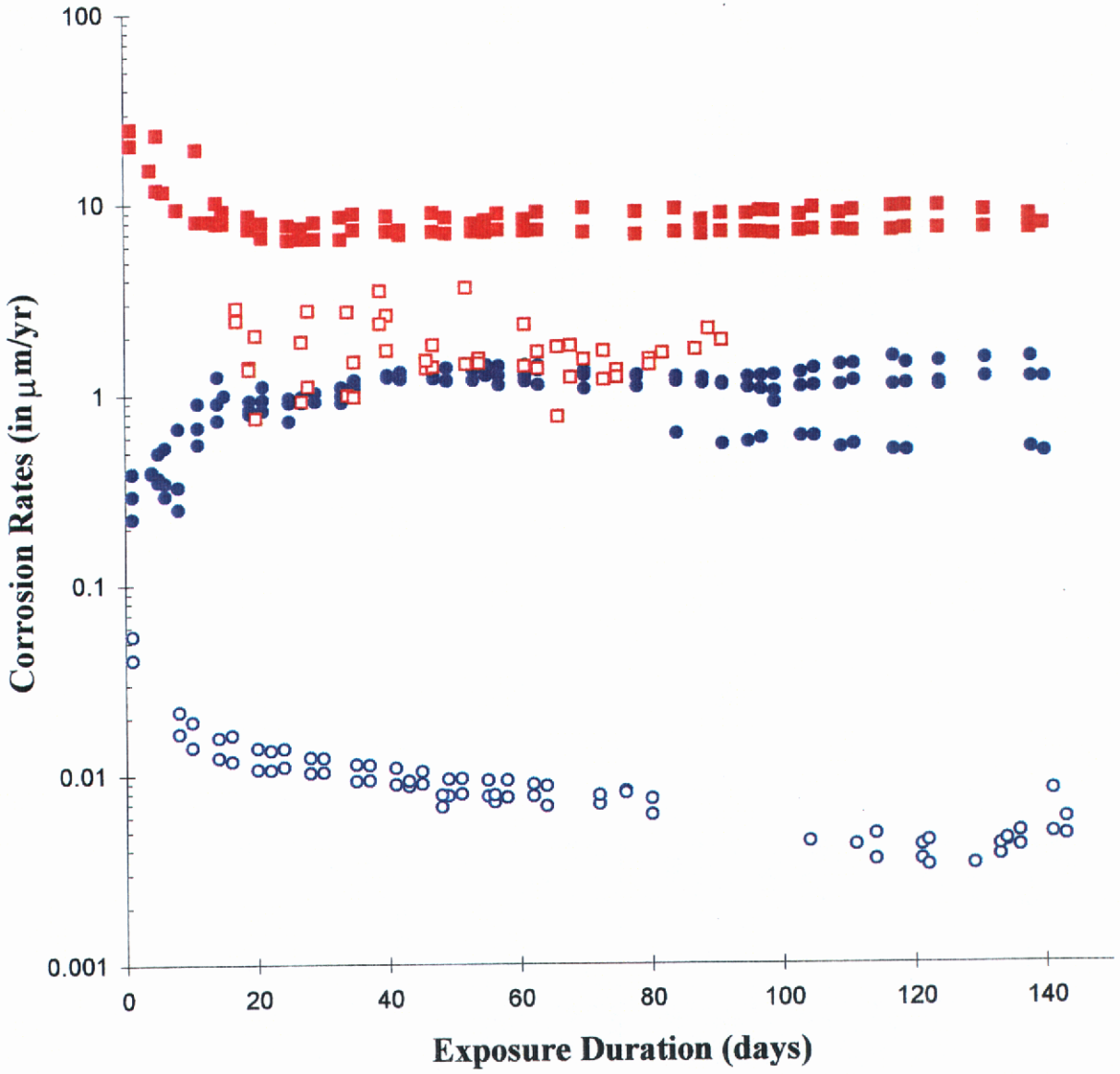

FIGURE 2: Influence of YM bacteria on corrosion rates of C1020 and M400. (■). C1020 inoculated with YM bacteria, (□). Sterile C1020; (●). M400 inoculated with YM bacteria; and (○). Sterile M400.

(a)

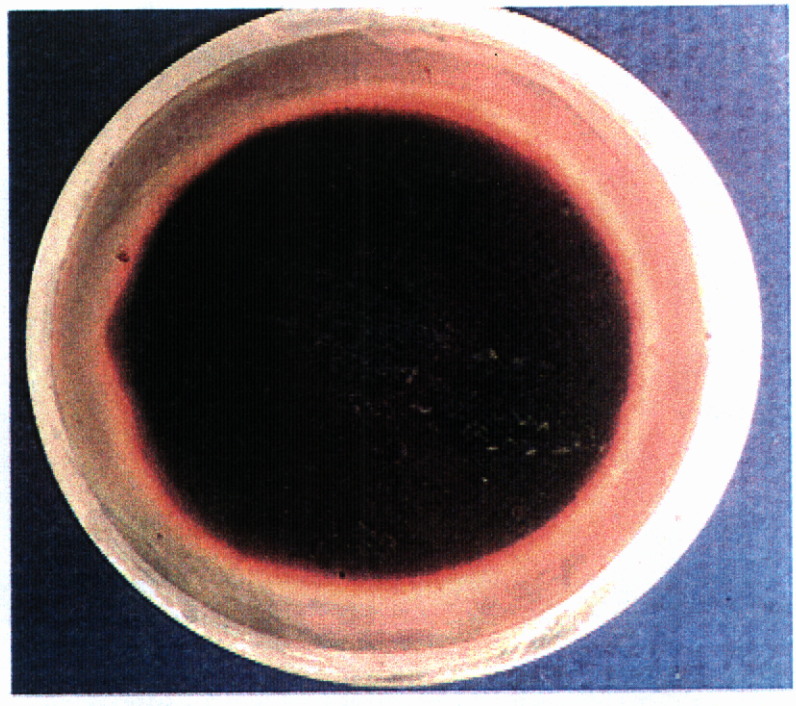

(b)

FIGURE 3: Gross appearance of M400 coupons after 5-month exposure in amended 100X J-13 water with YM bacteria, (a), and without YM bacteria, (b).

(a)

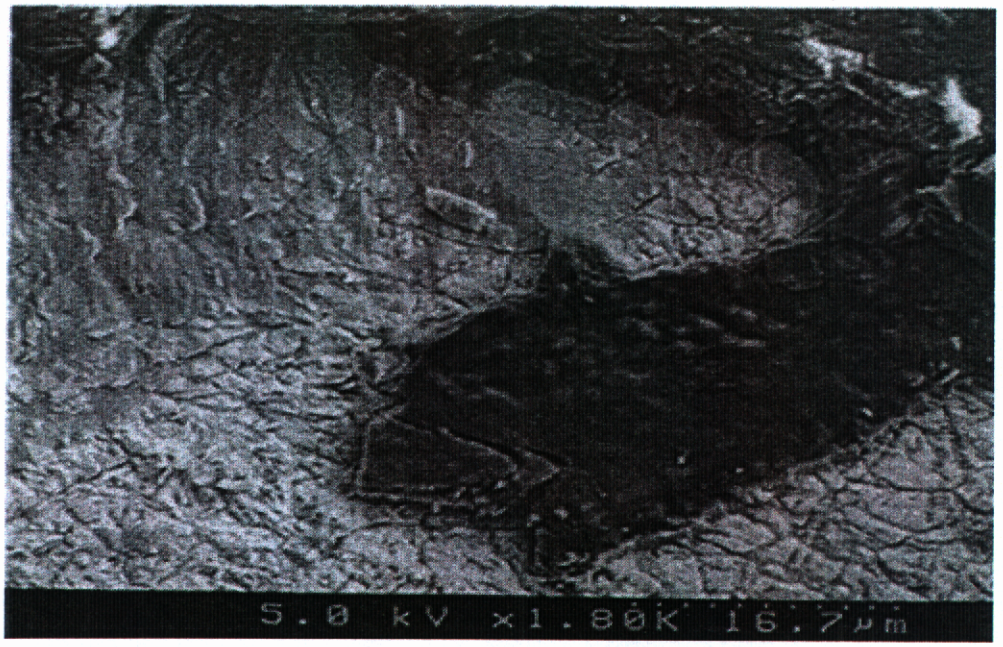

(b)

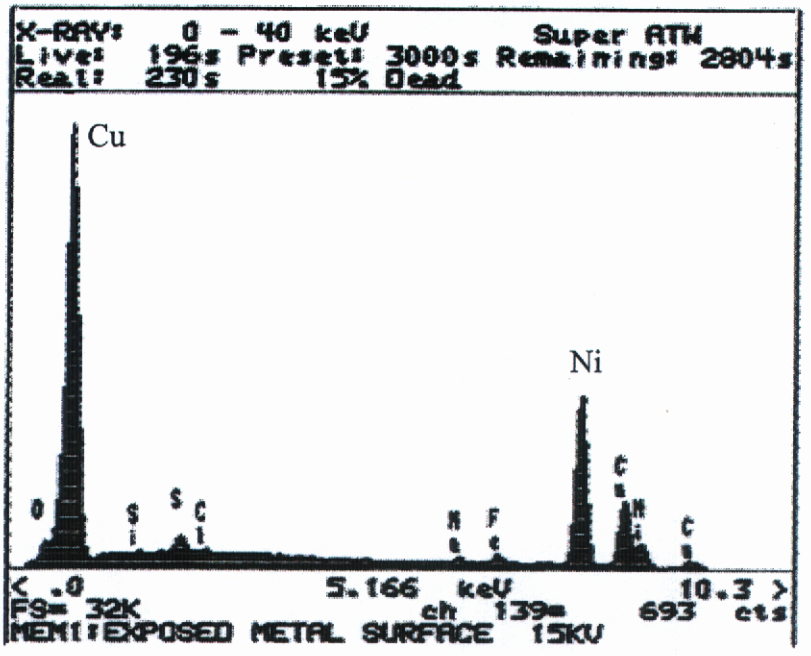

FIGURE 4: SEM image, (a), and EDAX spectrum, (b), of the surface of a M400 specimen coupon after 5-months exposure in the presence of YM microorganisms.

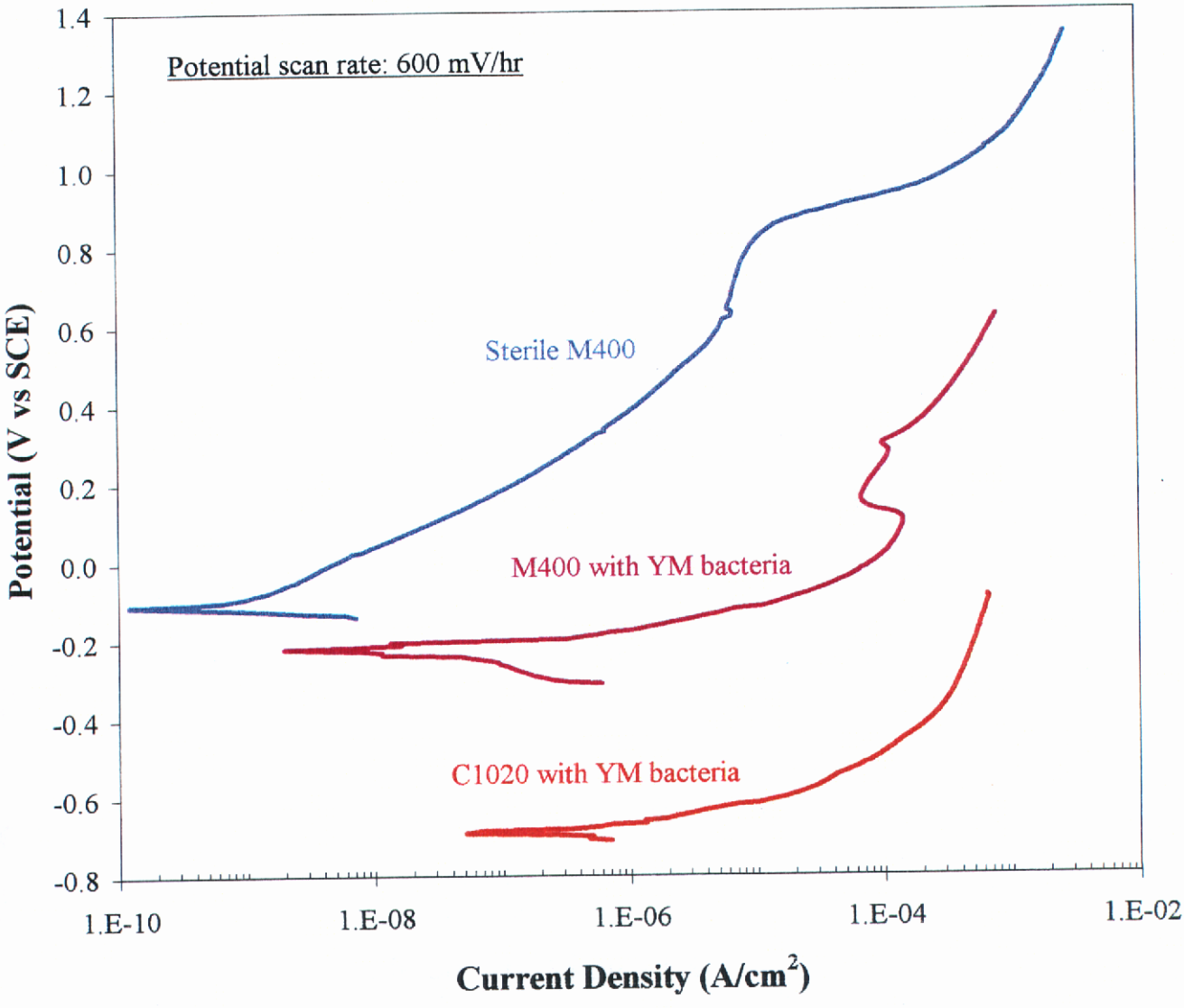

FIGURE 5: Comparison of anodic polarization behavior recorded on M400 with and without the presence of YM bacteria. The anodic polarization behavior of C1020 exposed to YM bacteria is also included for comparison.

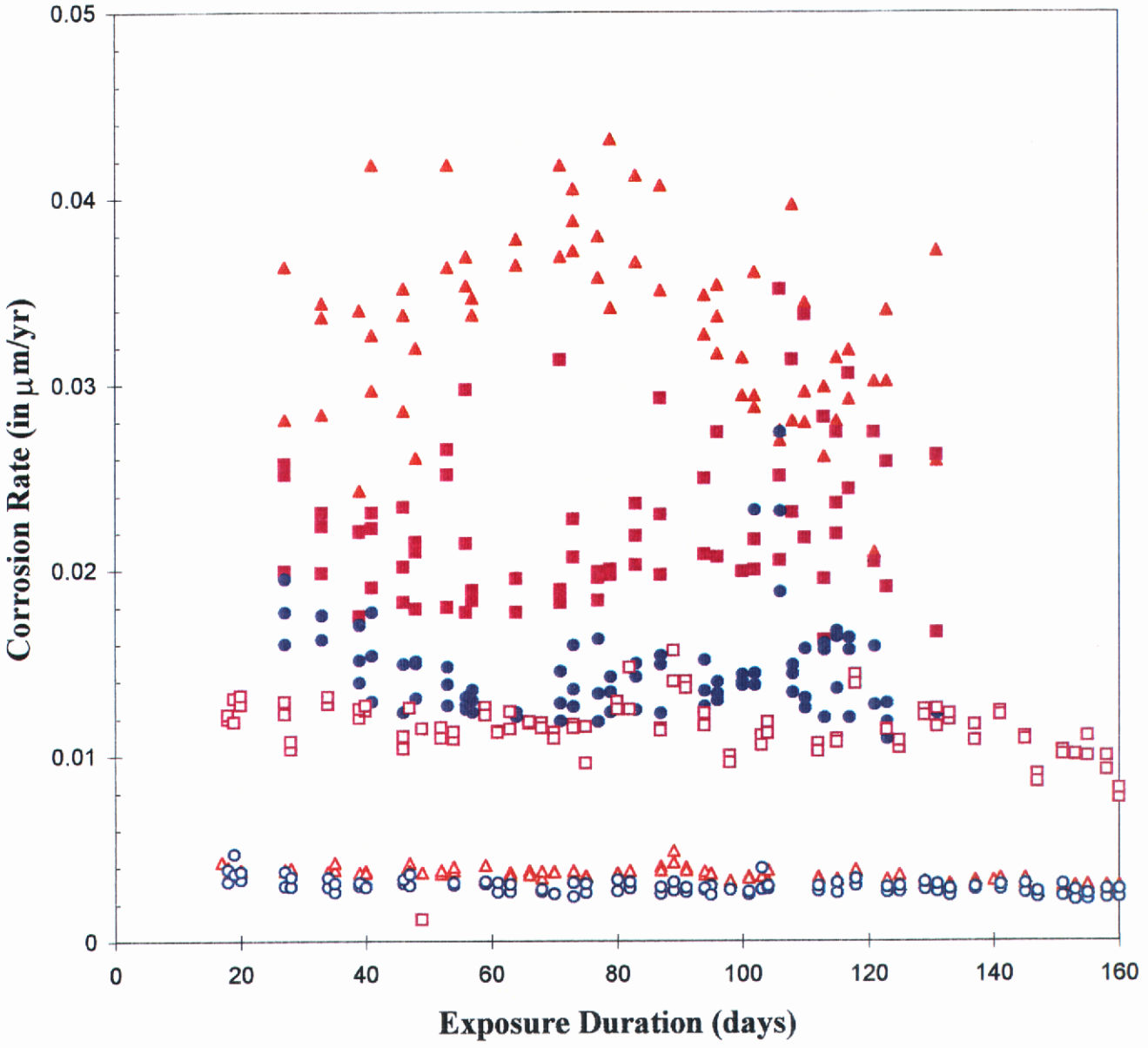

FIGURE 6: The influence of YM bacteria on corrosion rates of SS304, (▲) and (△), I625, (●) and (○), C-22, (■) and (□). MIC data, indicating incubation of test materials with YM bacteria, are shown by filled markers, and sterile data, indicating incubation in sterile systems, by open markers.

(a) 304SS

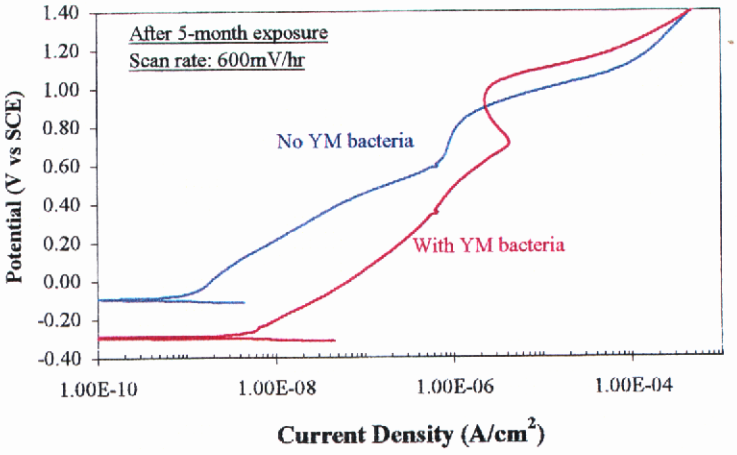

(b) I625

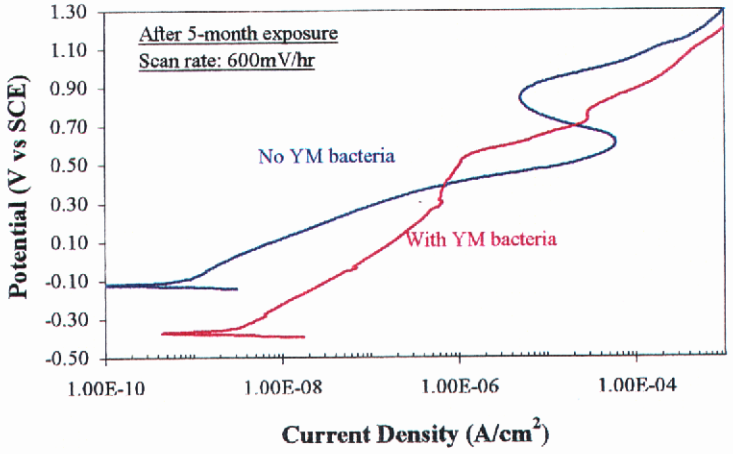

(c) C-22

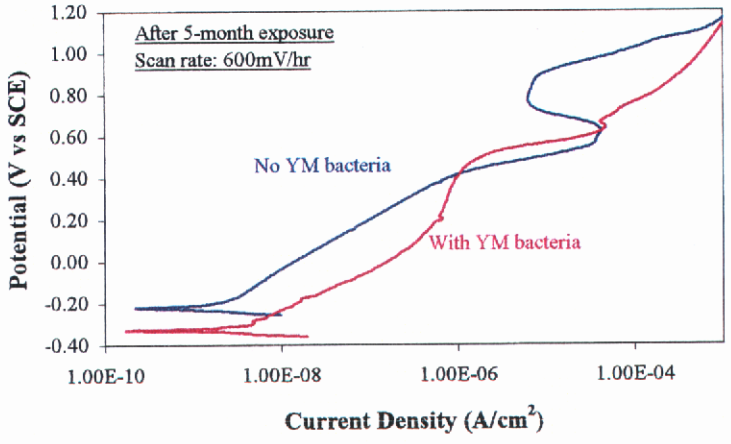

FIGURE 7: Anodic polarization behavior of 304SS, (a), I625, (b), and C-22, (c), exposed to amended J-13 well water with and without the presence of YM microorganisms.